Author/s:
Kwan, E;Legione, AR;Hartley, CA;Devlin, JM

Title:
Transcriptomic profiles of Crandell-Rees feline kidney cells infected with Varicellovirus felidalpha-1 (FHV-1) field and vaccine strains

Date:
2025

Citation:
Kwan, E., Legione, A. R., Hartley, C. A. & Devlin, J. M. (2025). Transcriptomic profiles of Crandell-Rees feline kidney cells infected with Varicellovirus felidalpha-1 (FHV-1) field and vaccine strains. Virology Journal, 22 (1), https://doi.org/10.1186/s12985-025-02722-w.

Persistent Link:
https://hdl.handle.net/11343/360514

Kwan *et al. Virology Journal* (2025) 22:102
https://doi.org/10.1186/s12985-025-02722-w

Virology Journal

RESEARCH Open Access

Transcriptomic profiles of Crandell-Rees feline kidney cells infected with *Varicellovirus felidalpha-1* (FHV-1) field and vaccine strains

Emily Kwan[1], Alistair R. Legione[1], Carol A. Hartley[1] and Joanne M. Devlin[1*]

Abstract

Background *Varicellovirus felidalpha-1* (FHV-1, previously *Felid alphaherpesvirus-1*) is a significant cause of upper respiratory tract disease in feline populations. Cats infected with FHV-1 show clinical signs that vary in severity. This can be due to differences in host responses and virus strain virulence. Investigating the gene transcription profiles during infections using FHV-1 strains could inform our understanding of host and viral factors contributing to disease outcomes. This study characterised the transcriptomes of Crandell–Rees feline kidney (CRFK) cells infected with field or vaccine FHV-1 strains to better understand the host response during infection.

Methods Crandell–Rees feline kidney cells were infected with either the FHV-1 F2 vaccine strain or the 384/75 field strain associated with severe disease. The transcriptomes were characterised using RNA-sequencing. To determine the host cellular transcription profile, the total transcripts were mapped to the cat genome and compared to uninfected cells. To characterise the viral transcription profile, the total reads were mapped to each FHV-1 strain. The differentially expressed host genes between infection strains were compared and further analysed using the PANTHER database to examine host pathway regulation.

Results The findings in this study show the differential host gene expressions induced by FHV-1 compared to uninfected CRFK cells. Genes encoding histone proteins were upregulated, while genes involved in cell adhesion and migration processes were downregulated during infections with FHV-1. Comparative analysis between field and vaccine strains showed similarities and differences in host gene expressions. Notably, upregulated genes unique to the field strain were associated with regulatory proteins involved in the cell cycle, while downregulated host genes in field and vaccine strains showed distinct host gene and pathway expressions involved in immune activation.

Conclusions This study demonstrates the host and viral gene expressions during FHV-1 infection shows the distinct host responses to field and vaccine strains using an in vitro model. These findings provide a foundation for future transcriptomic investigations in other cell types, including ex-vivo explants systems, to enhance our understanding of host and viral factors contributing to disease outcomes.

Keywords Feline herpesvirus-1, Upper respiratory tract disease, Feline viral rhinotracheitis, Transcriptomics, Virus-host interaction, Molecular pathogenesis

*Correspondence:
Joanne M. Devlin
devlinj@unimelb.edu.au

[1]Asia-Pacific Centre for Animal Health, Melbourne Veterinary School, Faculty of Science, The University of Melbourne, Building 400, Parkville, VIC 3010, Australia

Background

Feline viral rhinotracheitis (FVR) is a highly infectious upper respiratory tract disease (URTD) in cats caused by *Varicellovirus felidalpha-1* (FHV-1, previously *Felid alphaherpesvirus-1*). This enveloped double-stranded DNA virus is a member of the *Alphaherpesvirinae* subfamily and *Varicellovirus* genus [1]. Similar to other alphaherpesviruses, FHV-1 can establish latent infections in the trigeminal ganglion following primary FHV-1 infection [2]. During latency, cats do not present clinical signs or shed the virus. However, spontaneous viral reactivation can occur, resulting in viral shedding with or without clinical signs [3, 4]. Primary FHV-1 replication occurs in the mucosae of the eyes and upper respiratory tract, which can lead to clinical signs such as, rhinitis, conjunctivitis, and ocular ulcerations. In severe infections, FHV-1 can lead to blindness [5], pneumonia [6] and nonsuppurative meningoencephalitis [7]. Additionally, the presence of other viruses such as *Feline calicivirus* (FCV), can change FHV-1 infection outcomes and result in severe infections that lead to euthanasia [4, 8–10]. Analysis of FHV-1 strains show low genetic diversity (<0.01) which suggest genomic virulence determinates are unlikely related to host disease severity [11, 12].

The FHV-1 genome is 134 kbp, which encodes 78 open reading frames (ORFs) and 74 proteins [3, 13]. During viral replication, the synthesis of herpesvirus DNA occurs in the nucleus while protein synthesis takes place in the cytoplasm. Viral components either on the cell surface or within the cell can trigger immune responses during viral replication and many viral immune evasion strategies have been characterised to occur during alphaherpesvirus infections. Previous FHV-1 transcriptomic studies using RT-qPCR observed significantly increased nasal cytokine gene transcription in cats with FHV-1, which suggests host responses can contribute to FHV-1 pathogenesis and disease outcomes [14]. Several factors including the age, immune status and vaccination history of the cat, can contribute to the severity and outcome of FHV-1 infection. Investigating the transcriptomic response during FHV-1 infection may inform our understanding of host and viral factors contributing to viral pathogenesis and disease outcomes.

Table 1 FHV-1 isolates used in this study

Virus ID	Year of isolation	Genbank Acc. No.	Disease	Site
384/75	1975	KR381782 (12)	Pneumonia	Lung
356/75b	1975	KR381784 (12)	URTD[1]	N/A[2]
Feligen	1975	KR296657 (15)	N/A[2]	Vaccine
571/79	1979	KR381785 (12)	Conjunctivitis	Eye swab

[1] URTD = Upper respiratory tract disease

[2] N/A = Not applicable

Current FHV-1 vaccines are highly adapted to cell culture and are modified live-attenuated or inactivated forms of the F2 strain. The parent virus of the F2 strain was originally isolated in 1958 and attenuated through many passages in Crandell-Rees feline kidney (CRFK) cells at a low temperature [15]. Vaccinated domestic cat populations show effective protection against FHV-1 clinical signs. However, the impairment of the immune response by FHV-1 can increase the susceptibility to secondary infections and severe diseases [8]. Current FHV-1 vaccines can minimise the severity of clinical signs but do not prevent infection or the establishment of latent infections [3, 16]. Investigating the host and viral gene expressions during FHV-1 infections using strains that differ in virulence could shed light on the effects of viral strain virulence on host responses and infection outcomes. This study investigates the transcriptomes of CRFK cells infected with FHV-1 field or vaccine strains using an in vitro model to better understand host responses to FHV-1.

Methods

Virus selection and cell culture

Archived FHV-1 isolates of the F2 vaccine strain Feligen (Virbac New Zealand Ltd) and field strains that had been collected from cats with URTD were selected based on clinical signs and disease severity (Table 1) (Vaz et al., 2016). These isolates had 99.3% genetic identity using MAFFT whole genome alignment [17]. Monolayers of CRFK cells [18] were grown at 37°C in a humidified atmosphere of 5% v/v CO_2 in growth media containing Dulbecco's Modified Eagle basal media (DMEM, Sigma), 5% v/v foetal bovine serum (FBS, Sigma), 10 mM N-2-hydroxyethylpiperazine-N'-2- ethanesulfonic acid (HEPES) (pH 7.7) and antimicrobials (50 mg/mL ampicillin, 5 mg/mL amphotericin B).

Viral growth kinetics

One-step growth kinetics of each strain were determined in triplicate 6-well plates of CRFK cells. Uninfected cell monolayers at approximately 75% confluency were separately inoculated with each strain at a multiplicity of infection (M.O.I.) of 5 $TCID_{50}$ per cell. Uninfected control monolayers were mock inoculated with growth media only. After 1 h of incubation at 37 °C, the cell monolayers were washed twice with phosphate-buffered saline solution (PBS, pH 7.4, 137 mM NaCl, 8.2 mM Na_2HPO_4, 2.7 mM KCl) to remove the residual inoculum. Maintenance media containing DMEM with 1% v/v FBS, 10 mM HEPES pH 7.7 buffer solution and antimicrobials (50 mg/mL ampicillin, 5 mg/mL amphotericin B) were then added to each well. Samples were collected at six timepoints; 1-, 3-, 9-, 12-, 18- and 24-hour post-infection (h.p.i.) by freezing the plates at

– 80 °C. The material in each well was stored in 1 mL aliquots and used to determine the viral titres in CRFK cells by $TCID_{50}$ titration assays [19]. Statistical analysis of viral titres between FHV-1 strains at each time point was performed using Student's t-test, with P-values < 0.05 considered significant.

Sample Preparation for RNA sequencing

Inoculations of the Feligen vaccine strain and field strain 384/75 at an M.O.I. of 5 $TCID_{50}$ per cell were performed in 6-well plates of CRFK cells in triplicate and harvested at 6 h.p.i. for RNA isolation and sequencing. The supernatant was collected from the cell monolayers and stored in 1 mL aliquots at -80 °C. These samples were used to quantify viral titres by $TCID_{50}$ titration assays [19]. The cell monolayers were scraped from the wells and centrifuged at 300 × *g* for 5 min to remove the remaining supernatant. The pelleted material was resuspended in RLT Plus buffer (RNeasy Mini Kit, Qiagen) with 1% v/v β-mercaptoethanol and stored at – 80 °C. The total RNA was extracted using the RNeasy Plus mini kit (Qiagen), according to the manufacturer's instructions. The quality of RNA in each sample was quantified using the Agilent 4200 TapeStation system (Agilent Technologies, Santa Clara, CA). All samples showed RNA integrity numbers (RIN) > 8 and were used for Illumina RNA-sequencing.

Illumina RNA sequencing

Libraries of cDNA were constructed and sequenced at the Australian Genome Research Facility (AGRF, Melbourne). Briefly, the TruSeq stranded mRNA library preparation kit (Illumina Inc., San Diego) was used to construct cDNA libraries. Samples with the correct fragment size (~ 260 bp) were normalised to a sequencing depth of 20 million reads on the NextSeq 500 sequencing platform (Illumina Inc, San Diego) to produce libraries of 150 bp paired-end reads.

Quality control and processing of RNA-seq reads

Raw sequence reads were uploaded to the Galaxy web platform and analysed on the public server *usegalaxy.org* to assess the read quality using FastQC version 0.11.8 [20, 21]. Adapter sequences and low-quality reads were trimmed using CutAdapt [22, 23]. The high-quality reads were mapped to the annotated domestic cat genome 126 version 1 [24] (general feature format and FASTA format), obtained from the NCBI database (Genbank accession no. GCF_018350175.1), to determine host transcription. The total reads from each library were also mapped to the FHV-1 field strain 384/75 genome [12] (Genbank Accession No. KR381782) to compare viral transcripts between field and vaccine strains. Both host and viral read mapping was performed using RNAstar [25].

Differential gene expression analysis

The host and viral counts per gene were normalised and converted to $\log_2$ counts per million (CPM) on the interactive RNA-seq analysis platform Degust using Voom/Limma version 4.2 [26–28]. Significant changes to gene expression were filtered in the RStudio environment version 2023.06.1 + 524 using the $\log_2$ fold changes (LFC) that met the following conditions: (i) genes must have greater than 10 CPM reads in at least one treatment group, (ii) the LFC must be greater than 2 (or less than – 2), and (iii) the false discovery rate (FDR) of genes must be < 0.05. Analyses of viral gene expression were performed on Geneious Prime 2023.0.1.

Categorisation of host genes with gene ontology

Differential host gene expression was further analysed on the online PANTHER database version 17.0 to identify enriched gene ontology (GO) terms that were retrieved from the Uniprot database [29]. The protein-encoding genes of the cat were extracted, indexed and linked to the differentially expressed host genes to analyse pathway regulation by biological function [30]. Statistical enrichment analysis on the differentially expressed genes was categorised by molecular function, cellular component, and biological processes with P-values < 0.05 considered significant [31].

Sample Preparation for UL32 RT-qPCR

To further investigate FHV-1 UL32 expression, CRFK cells were infected and harvested as described for viral growth kinetics. At each timepoint, the cell monolayers were scraped from the wells and centrifuged at 300 × *g* for 5 min to remove the supernatant. The pelleted material was resuspended in RLT buffer with 1% v/v β-mercaptoethanol and stored in 1 mL aliquots at – 80 °C. The total RNA was extracted using the RNeasy Plus mini kit and converted into cDNA using the SuperScript III reverse transcriptase kit (Invitrogen), following the manufacturer's instructions. The cDNA of each triplicate across the six timepoints was stored at – 80 °C and quantified using RT-qPCR.

Preparation of standards for UL32 RT-qPCR

Field strain 384/75 was used to generate standard curves for UL32 RT-qPCR transcription analysis. The total RNA was extracted using the RNeasy Plus mini kit and converted into cDNA using the Superscript III reverse transcriptase, according to the manufacturer's instructions. The concentration of cDNA was determined using the Qubit RNA Broad Range Assay kit (Invitrogen) and serially diluted 10-fold from 10^8 to 10^2 copies per µL in triplicate with nuclease-free water.

FHV-1 RT-qPCR

Primer sets for UL32 and UL33 genes were designed to produce 150 bp products. Each 20 µL reaction was performed in the AriaMx Real-Time PCR system (Agilent Technologies) and contained 0.17 mM of either UL32 or UL33 primers (Table 2), 0.2 mM of each dNTP, 2 mM $MgCl_2$, GoTaq colourless buffer (Promega), 8 mM Syto 9 (Life technologies), 1 U GoTaq Flexi DNA polymerase (Promega) and 3 µL of cDNA template. Negative control reactions containing DNA-free water instead of cDNA template were included in triplicate. Initial denaturation was performed at 95 °C for 3 min, followed by 35 cycles of denaturation at 95 °C for 30 s, annealing at 58 °C for 30 s and extension at 72 °C for 20 s. A melt curve was produced by heating the amplified product from 72 to 95 °C, increasing by 0.2 °C every second, to confirm the correct product was amplified. The genome copies in each sample were determined using the AriaMx Real-Time PCR software and the UL32 transcription was normalised to the neighbouring upstream gene UL33 at each timepoint for field and vaccine strains. The UL33 gene is conserved amongst alphaherpesviruses and transcribes independently to UL32. The relative UL32 expression in the vaccine infection group at each timepoint was compared to the field infection, using Student's t-test with P-values < 0.05 considered significant.

Table 2 Primers used for UL32 FHV-1 RT-qPCR

Primer	Direction	Sequence (5′ → 3′)	Binding site (nt)[1]
UL32	Forward	CCATACCACTCTGTGCCACC	46,212–46,231
	Reverse	GAACGCCCCCACCAAAGTAA	46,318–46,299
UL33	Forward	AACGTGATTTTTGCGTGGCC	45,525–45,544
	Reverse	TTATCATATACCCAGCGACTCG	45,624–45,603

[1] Nucleotide numbers of the binding site relate to the alignment of the FHV-1 F2 vaccine strain (Feligen) (Genbank Accession No. KR296657)

Results

Growth kinetics of FHV-1 field and vaccine strains

The growth curves of the different FHV-1 strains were similar over 24 h (Fig. 1). Cytopathic effects (CPE) were observed in cells infected with FHV-1 from 6 h.p.i. Statistical analysis of viral titres between FHV-1 isolates showed significantly higher titres of field strain 356/75b compared to the vaccine strain at 1 and 18 h.p.i. ($P = 0.04$ and $P = 0.02$, respectively) and significantly higher titres than field isolate 571/79 ($P = 0.02$) at 3 h.p.i. and 384/75 ($P = 0.02$) at 24 h.p.i. Field isolate 384/75 showed significantly lower viral titres than isolate 356/75b at 12 h.p.i. ($P = 0.03$). No CPE was observed in the uninfected cells at any time point.

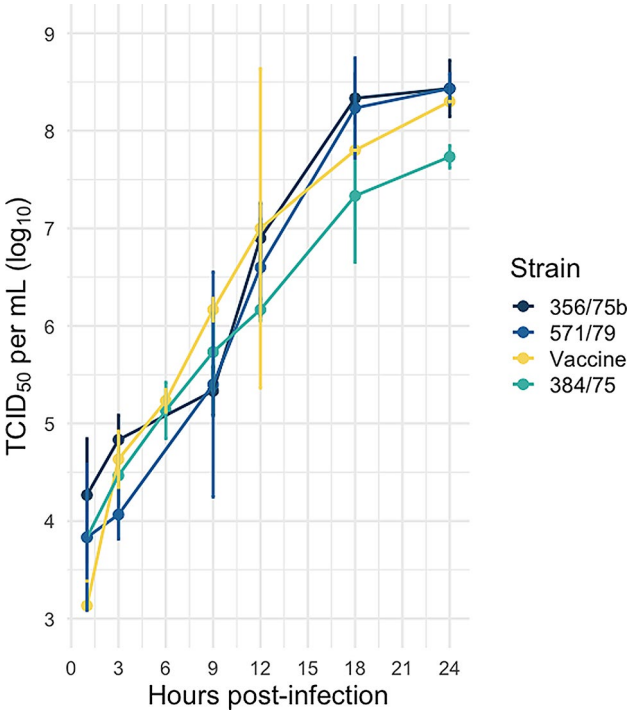

Fig. 1 One-step growth curves of FHV-1 field and vaccine strains in CRFK cells infected in triplicate an M.O.I. of 5 $TCID_{50}$ per cell. Viral titres at each timepoint were determined using $TCID_{50}$ assays and the mean $TCID_{50}$ titre across triplicates is shown. Error bars represent the standard deviation

Host and viral RNA are distinguishable in FHV-1 infections in vitro

High-quality reads across the infection groups mapped to the domestic cat genome. In samples infected with FHV-1 field or vaccine strains, the total reads also mapped to the genome of the field strain 384/75 (Fig. 2). The principal component analysis (PCA) plot generated using the $\log_2$ CPM values of the total reads mapped to the cat genome showed minimal variation between the triplicates of FHV-1 infection groups and a distinct difference between the infection groups and uninfected samples (Supplementary Fig. 1). The data from this study has been deposited to the NCBI BioProject database under BioProject accession number PRJNA1082348.

Field and vaccine strains show minimal differences in viral gene transcription

Viral reads in the FHV-1 infection groups mapped to the complete FHV-1 genome consisting of 73 viral genes. The transcript per million (TPM) of each FHV-1 gene is shown in Fig. 3. Differential viral gene expression analysis of the vaccine strain compared to the field strain showed a significant difference in UL32 gene transcription with an LFC of 2.16 ($P < 0.01$) (Supplementary Fig. 2).

Further examination of UL32 transcription in CRFK cells infected with FHV-1 field or vaccine strain, using RT-qPCR, did not show significant differences in relative UL32 expression, compared to UL33, across timepoints between field and vaccine strains. The average

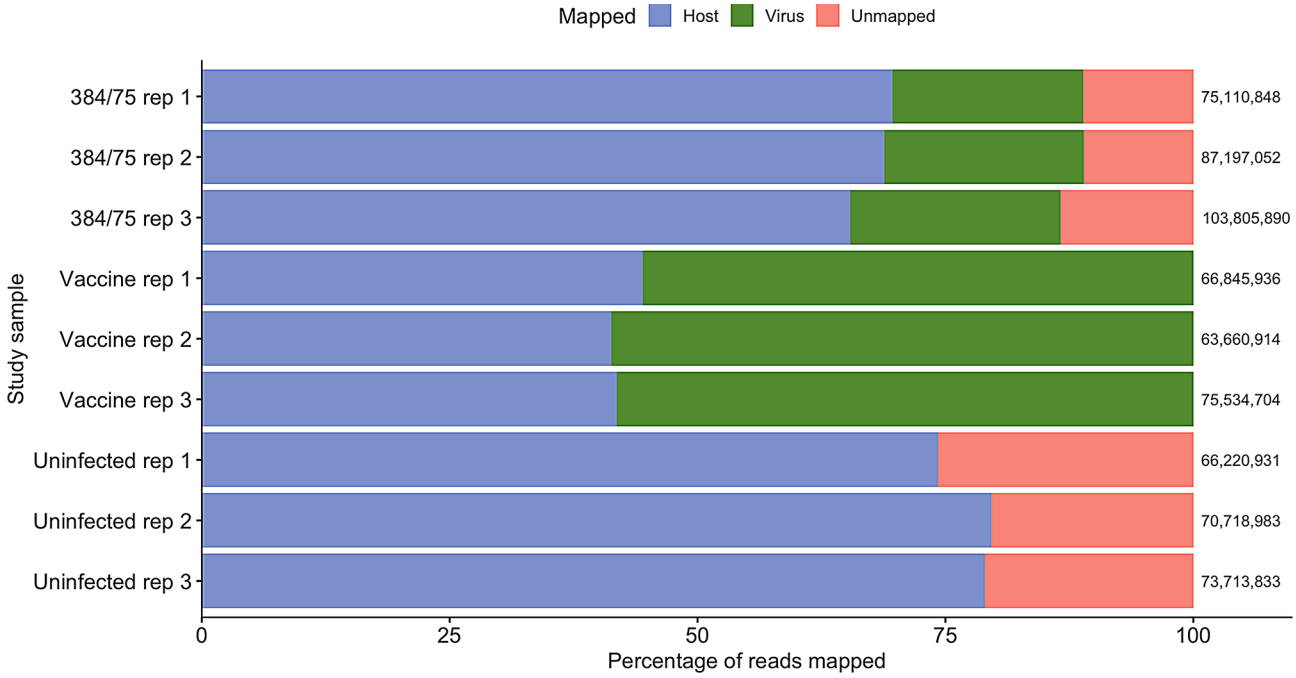

Fig. 2 Percentage of the total reads that mapped to the domestic cat genome Fca126 (RefSeq acc. GCA_018350175.1) and FHV-1 field strain 384/75 genome in each replicate (rep) of uninfected cells and cells infected with field strain (384/75) or vaccine strain (Vaccine). The total number of reads of each sample is shown at the right end of each sample. The unmapped reads are also shown

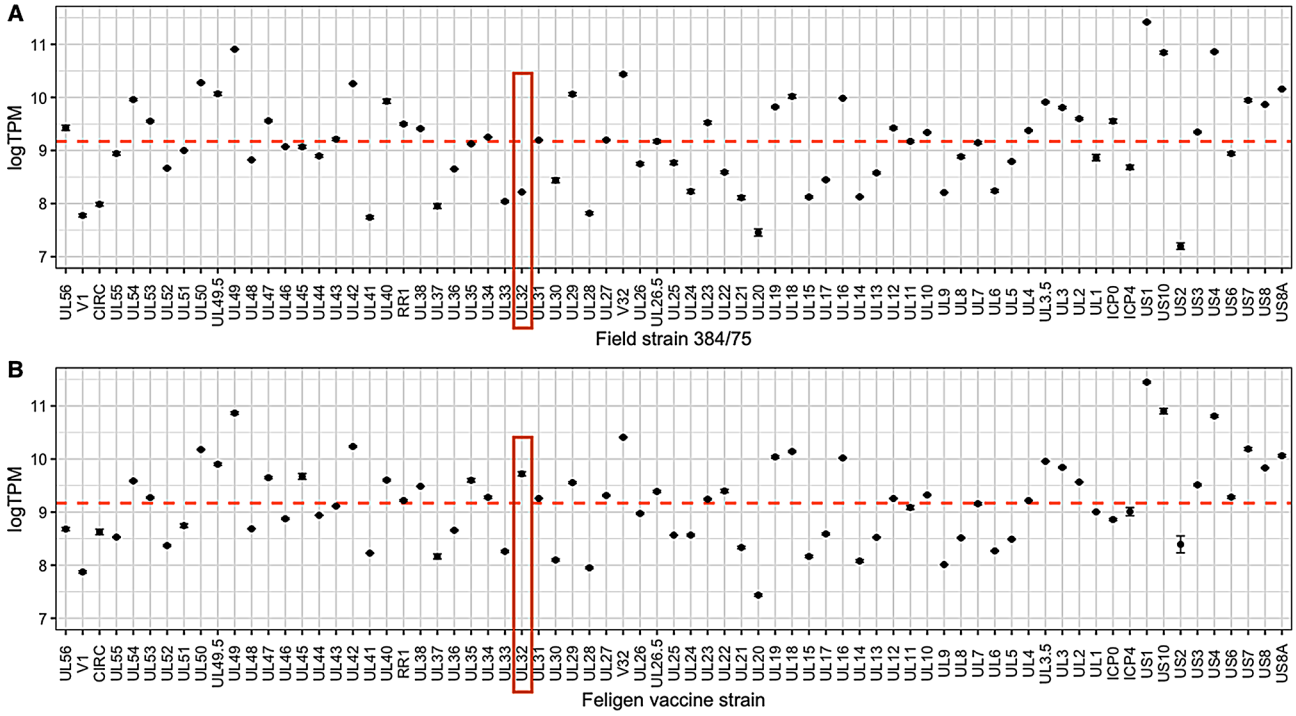

Fig. 3 (**A**) The $\log_{10}$ transcript per million (logTPM) count of FHV-1 384/75 genes in CRFK cells. (**B**) The logTPM count of FHV-1 vaccine genes in CRFK cells. The median TPM across the genome is shown in red and the order of genes presented represents the order of the genes in the genome. The transcription of UL32 in field and vaccine strains is highlighted in red

copy numbers of UL32 and UL33 transcripts in samples infected with field or vaccine strains are shown in Fig. 4.

Field and vaccine FHV-1 strains induce changes to host cellular gene expression

The total host reads in the field and vaccine infection group compared to the uninfected samples showed differentially expressed host genes (Fig. 5). Cells infected with the field strain 384/75 showed a total of 1,024 differentially expressed genes compared to uninfected cells, of which 837 were upregulated and 187 were downregulated. In cells infected with the vaccine strain, 2,823 genes were differentially expressed. Of these 2,500 genes were upregulated and 323 genes were downregulated.

Differentially expressed host genes between field and vaccine strains

A comparison of the differentially expressed host genes in the field and vaccine infection groups showed 795 genes that were identified in both infection groups (Fig. 6). Of these, 682 were upregulated and 113 were downregulated. The remaining genes differentially expressed in each infection group showed the vaccine infection group with ten times more differentially expressed genes than the field infection group. The top 10 commonly up- and downregulated genes showed similar changes in host gene expression between field and vaccine infection groups, compared to uninfected cells (Table 3). Genes encoding histone proteins dominated the top 10 upregulated gene, accounting for eight upregulated genes in both infection groups. The top 10 downregulated genes common to both infection strains dysregulated cell surface and pattern recognition receptors, as well as genes regulating cell adhesion, migration and division processes associated with immune responses.

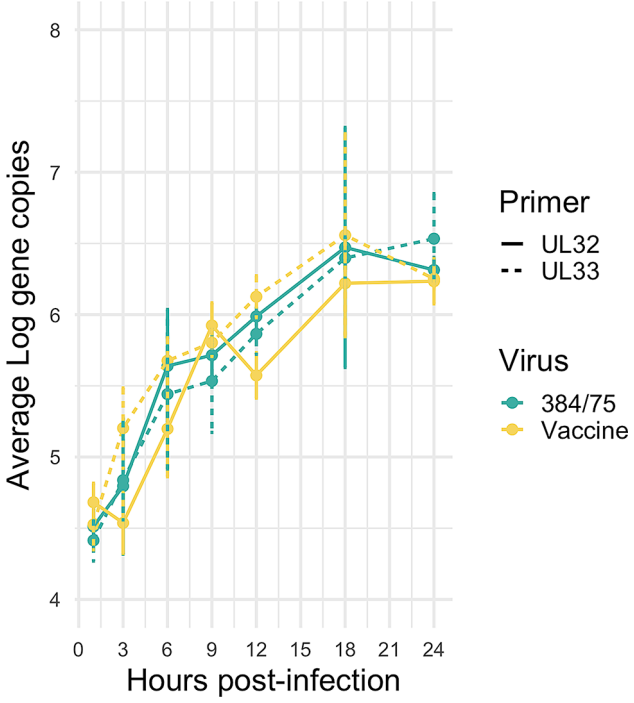

Fig. 4 The average genome copies of UL32 and UL33 transcripts in CRFK cells infected with field or vaccine FHV-1 strains using RT-qPCR. Error bars representing the standard deviations of each replicate at each timepoint are shown

Host gene expressions can differ between field and vaccine FHV-1 strains

The top 10 up- and downregulated genes unique to each infection group showed higher changes in LFC expression levels in cells infected with the vaccine strain than the 384/75 field strain (Table 4). The LFC values of these genes were generally lower than the genes common between the infection groups described in Table 1. The highest upregulated genes uniquely differentially expressed in the field infection group were associated with tRNA species and regulatory proteins involved in the cell cycle. The characterised downregulated genes were involved in the expression of transmembrane proteins, binding proteins, and regulators of the immune response. The greatest upregulated genes uniquely differentially expressed in samples infected with the vaccine strain were small non-coding RNA. The most downregulated genes were associated with kinase expression, transmembrane cell signalling protein, cellular metabolism, and inflammatory responses.

Field and vaccine FHV-1 strains enriched genes with different host functions

The significant differentially expressed host genes in the FHV-1 infection groups were linked to GO terms that categorise the differentially expressed genes based on their roles in cellular components, molecular functions, and biological processes. The enriched GO terms in field and vaccine infection groups showed differences within each functional group category and more enriched GO terms in cells infected with the field strain compared to the vaccine strain (Fig. 7). Infections using the vaccine strain induced more changes to host gene expression and pathway regulations than the field strain but enriched fewer host pathway functions. Independent enrichment analysis of the upregulated and downregulated genes in samples with FHV-1 infections did not show significantly enriched GO terms across most functional categories. Samples infected with the field strain showed an exception, with 27 upregulated genes enriched in DNA binding molecular function.

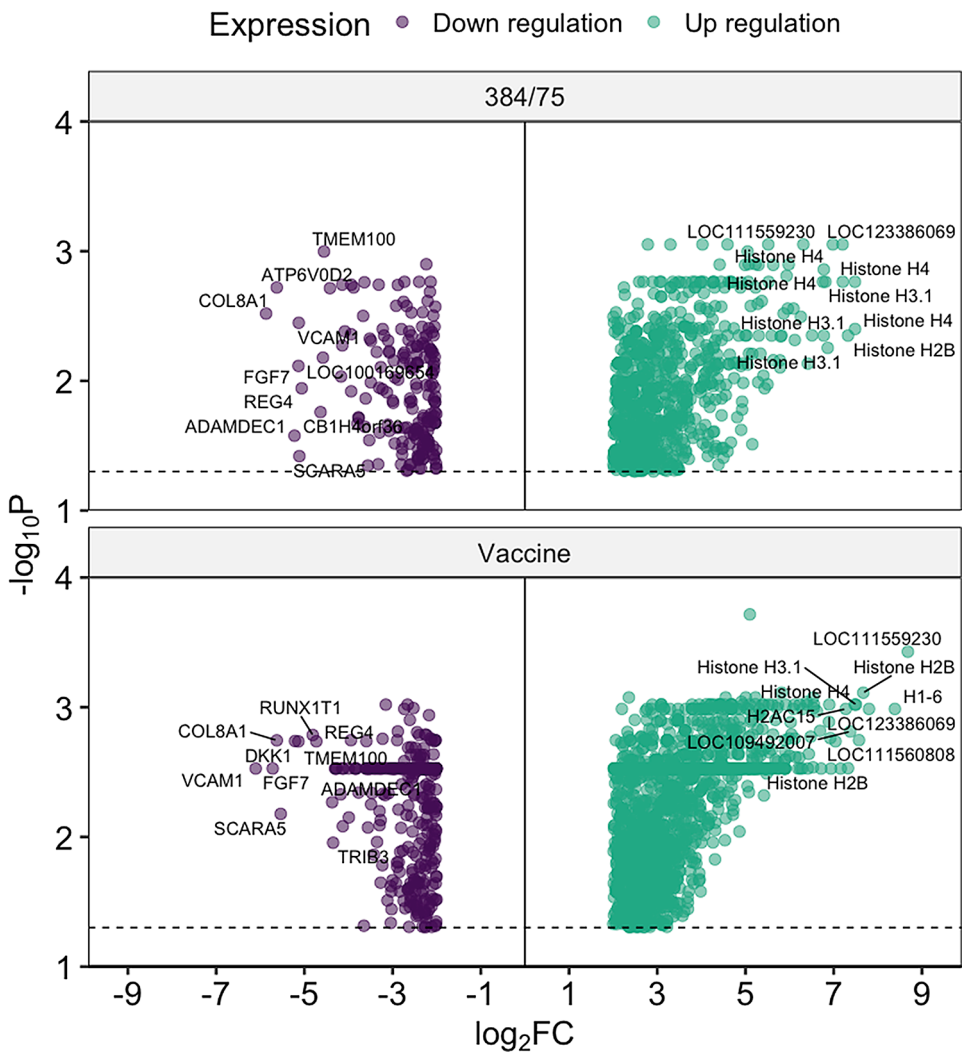

Fig. 5 Volcano plots of the total significantly expressed up- and downregulated host genes in CRFK cells infected with the field strain 384/75 or the vaccine strain (Feligen). Host gene expression in the FHV-1 infected samples was compared to the uninfected cells. The top 10 up- and downregulated genes are labelled

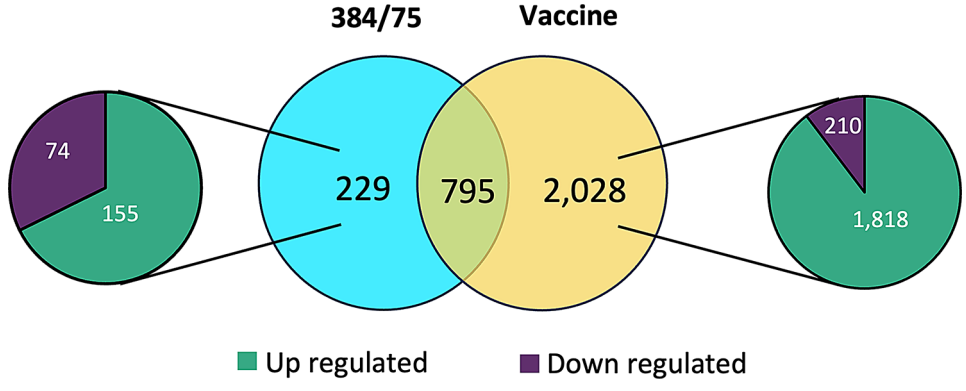

Fig. 6 The number of host genes differentially expressed in both infection groups and unique to each infection group are shown (blue and yellow circles). The total number of up- and downregulated genes unique to samples with field and vaccine infections are shown alongside each infection group (purple and green circles)

Table 3 The top 10 commonly up- and downregulated genes in CRFK cells inoculated with the field (384/75) or vaccine (Feligen) strain

Up regulated	Gene ID	Gene function	384/75		Vaccine	
			FDR[1]	LFC[2]	FDR[1]	LFC[2]
	H4C16	Histone	< 0.01	7.48	< 0.01	7.16
	H4C13	Histone	< 0.01	7.48	< 0.01	6.92
	H2BC3	Histone	< 0.01	7.32	< 0.01	7.32
	H3C11	Histone	< 0.01	7.21	< 0.01	7.80
	LOC123386069	–	< 0.01	7.20	< 0.01	7.80
	LOC111559230	–	< 0.01	6.98	< 0.01	8.68
	H3C6	Histone	0.01	6.86	< 0.01	6.94
	Histone H4	Histone	< 0.01	6.81	< 0.01	7.48
	Histone H4	Histone	< 0.01	6.78	< 0.01	6.62
	Histone H3.1	Histone	< 0.01	6.77	< 0.01	6.71
Down regulated	COL8A1	Cell homeostasis	< 0.01	-5.87	< 0.01	-5.63
	ATP6V0D2	Cell adhesion	< 0.01	-5.63	< 0.01	-4.00
	ADAMDEC1	Cell migration	0.03	-5.22	0.01	-4.37
	FGF7	Growth factor	0.01	-5.13	< 0.01	-5.72
	VCAM1	Cell surface receptor	0.00	-5.13	< 0.01	-6.10
	SCARA5	Pattern recognition receptor	0.04	-5.11	0.01	-5.54
	REG4	Cell homeostasis	0.01	-5.06	< 0.01	-4.73
	CB1H4orf36	–	0.02	-4.63	0.01	-2.20
	MHC class II	Cell surface receptor	0.01	-4.58	< 0.01	-2.17
	TMEM100	Cell homeostasis	< 0.01	-4.56	< 0.01	-5.14

[1] The false discovery rate (FDR) is shown

[2] P-values < 0.05 with LFC > 2 for upregulated or < -2 for downregulated genes were considered significant

The functions of characterised genes are shown alongside the gene expression levels, which are represented by $\log_2$ fold change (LFC), ordered by expression in field infection samples

Table 4 Top 10 up- and downregulated genes uniquely expressed in CRFK cells infected with the FHV-1 field strain (384/75) or vaccine strain (Vaccine)

Up regulated	Gene ID	384/75		Gene ID	Vaccine	
		FDR[1]	LFC[2]		FDR[1]	LFC[2]
	LOC111560238	0.04	4.29	SNORD58	< 0.01	5.71
	LOC109499602	0.02	3.47	SNORA3/45	< 0.01	5.52
	TRNAW-CCA_8	0.04	3.44	LOC123384631	< 0.01	5.47
	TRNAF-GAA_10	0.01	3.43	SNORD14	< 0.01	5.45
	LOC109491671	0.02	3.42	LOC109502106	< 0.01	5.45
	LOC109500935	0.01	3.38	LOC111561262	< 0.01	5.35
	LOC101088630	0.02	3.29	LOC111561932	< 0.01	5.32
	SFN	0.05	3.22	SNORD22	< 0.01	5.18
	LOC111560944	0.01	3.19	LOC123385372	< 0.01	5.13
	LOC109493372	< 0.01	3.19	LOC109501215	< 0.01	5.10
Down regulated	TMEM26	0.02	-3.77	TRIB3	0.01	-4.35
	INHBE	0.01	-3.49	LOC109503125	0.01	-4.13
	FABP7	0.03	-3.30	LOC101096785	0.01	-4.00
	LOC109491403	0.01	-3.20	XPNPEP2	0.05	-3.65
	LOC123380486	0.02	-3.11	LOC111556196	0.01	-3.56
	LOC111558401	0.01	-3.10	EDNRA	0.01	-3.42
	LOC123383220	0.01	-3.08	DUOX2	< 0.01	-3.42
	LOC109503254	0.02	-2.99	LOC102899057	< 0.01	-3.40
	LOC123383127	0.01	-2.98	HLF	< 0.01	-3.34
	LOC109500446	0.03	-2.95	LOC101085945	< 0.01	-3.31

[1] The false discovery rate (FDR) is shown

[2] P-values < 0.05 with LFC > 2 for upregulated and LFC < -2 for downregulated were considered significant

Gene expression levels are represented by $\log_2$ fold change (LFC) and were compared to uninfected samples across triplicates

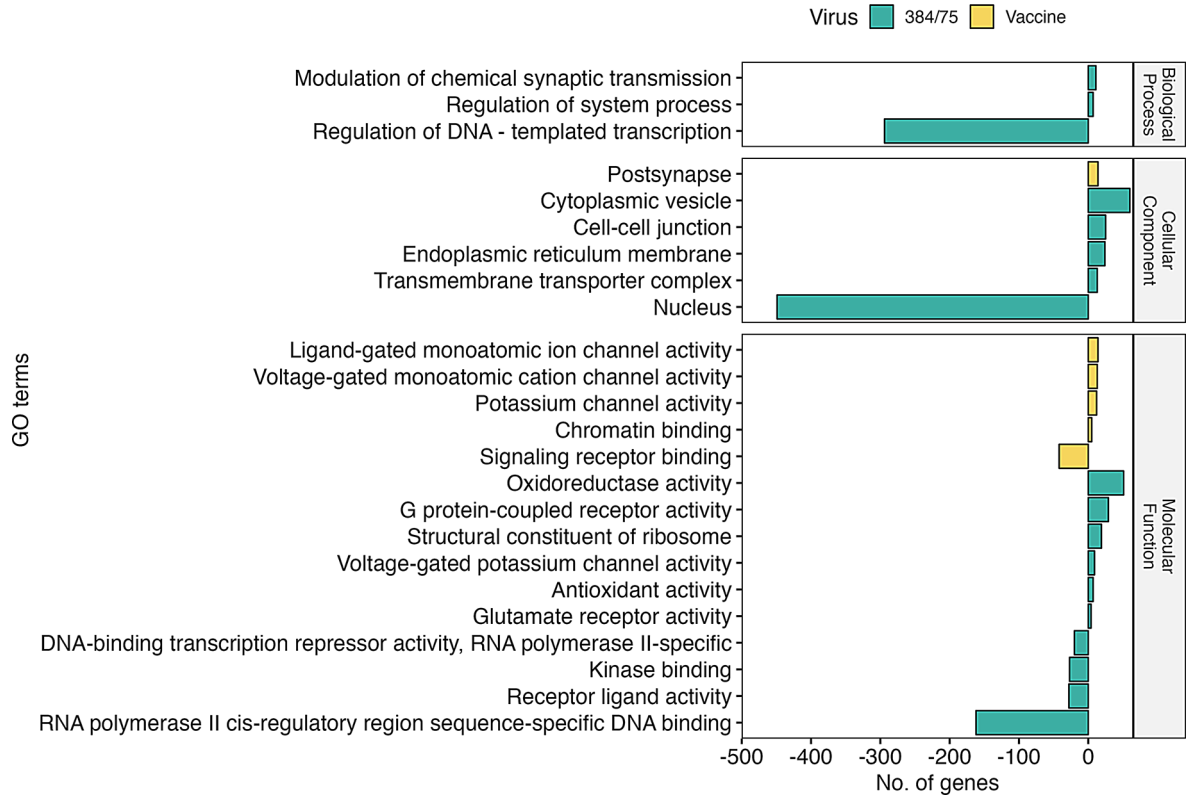

Fig. 7 Statistical enrichment analysis of the total up- and downregulated protein-encoding genes in the field and vaccine infection groups by biological process, molecular function, and cellular components. Overrepresented GO terms are shown > 0 and the underrepresented GO terms are shown < 0. The number of enriched genes that contributed to each pathway is shown

Field and vaccine FHV-1 strains regulated different host pathways

The differentially expressed host genes in samples infected with the vaccine strain regulated more host proteins and pathways than cells infected with the field strain. Infections with the vaccine strain contributed to 224 protein-encoding genes which regulated 76 pathways, compared to 93 genes in the field strain regulating 48 pathways (Supplementary Fig. 3). Comparative analysis of host proteins and pathways between field and vaccine strains showed the expression of 34 unique protein-encoding genes in samples infected with the vaccine strain, which contributed to 24 dysregulated pathways (Fig. 8).

Discussion

The host and viral transcription profiles of CRFK cells infected with field or vaccine FHV-1 strains were analysed at 6 h.p.i. At this timepoint, viable cell monolayers showed early signs of CPE due to FHV-1. This indicated active viral replication and cellular mRNA transcription in the infected cell cultures. Feline kidney cells are epithelial cells, which are highly susceptible to FHV-1 infections and do not have immune function. This allows the findings of this study to demonstrate the host response during FHV-1 infections in a homogenous cell population from the natural host. By characterising the transcriptomes of cells infected with the F2 vaccine strain or 384/75 field strain, associated with severe URTD, this study explored the potential impact of viral strain virulence. Infections of CRFK cells with field and vaccine FHV-1 strains induced significant changes to host gene expression when compared to uninfected cells. Histone genes were strongly represented in the top 10 upregulated genes in CRFK cells infected with field or vaccine strains, while genes associated with cell adhesion and immune activation were downregulated. Comparative analysis of host transcription profiles between field and vaccine strains showed similarities and differences in host gene expression, with some genes associated with immunoregulation distinctly expressed during infection with each FHV-1 strain. The findings in this study show the host and viral gene expressions during infections using field or vaccine FHV-1 strains, which demonstrates the different host responses associated with viral strain virulence.

Histone genes were upregulated during FHV-1 infections, compared to uninfected cells, which is consistent with previous studies using herpes simplex virus type 1 (HSV-1) [32–34]. Histones are structural proteins

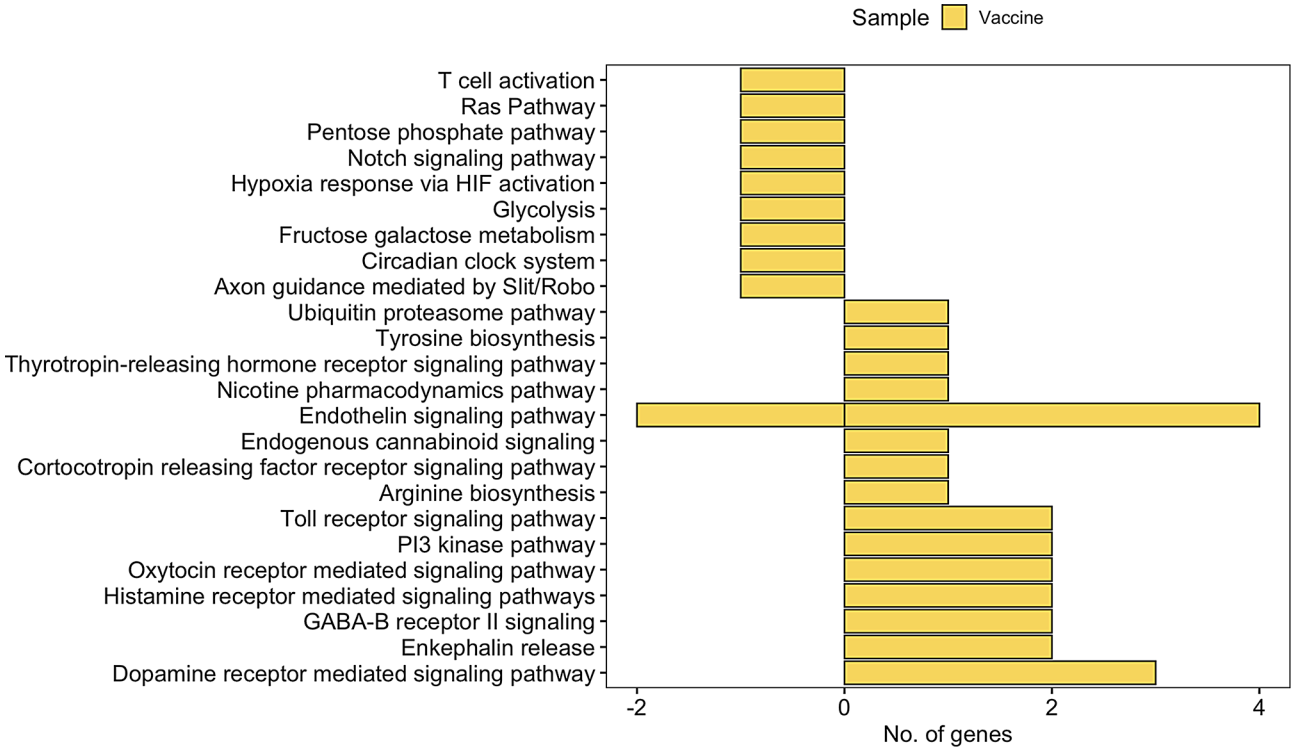

Fig. 8 Host pathways uniquely regulated in CRFK cells infected with the vaccine strain compared to cells infected with the field strain. The number of upregulated protein-encoding genes contributing to host pathways are shown > 0 and the downregulated genes are shown < 0

that package DNA within the cell nucleus and form the nucleoprotein complex, chromatin. The upregulation of histone genes in this study highlights the interactions between histones and the viral genome, which are well-characterised in alphaherpesviruses [35]. Upon viral entry into the nucleus, herpesvirus DNA can bind to histones and induce modifications to the structure of host chromatin, which can activate the expression of precursor histones. Host repair factors and DNA damage responses are associated with chromatin modifications, which could suggest host DNA repair pathways may be activated during herpesvirus infection [36].

Cell surface receptors and growth factors associated with innate immune activity were downregulated during FHV-1 infections compared to uninfected cells. This finding is consistent with previous HSV-1 transcription studies in epithelial cells which observed changes in host pathways regulating cell adhesion and migration, and immune activation [37]. Cell surface and pattern recognition receptors have roles regulating cell adhesion and migration, including the recruitment of leukocytes, such as macrophages and T-cells [38, 39]. Additionally, cellular growth factors involved in cell injury responses can influence cell differentiation and division processes which contribute to inflammation and repair. In cats with FHV-1 infections, RT-qPCR analysis observed significantly increased chemokines and cytokines, including tumour necrosis factor (TNF)-α, interleukin (IL) -6, -10, and interferon (IFN)-γ mRNA transcription, which can activate cell surface receptors [14]. The downregulated genes in cells infected with FHV-1 is consistent with previous in vitro studies, which show FHV-1 can influence immunoregulation and downregulate the surface expression of major histocompatibility complex (MHC) class II proteins [40]. These findings highlight the viral immune evasion strategies, which are well characterised in alphaherpesviruses, can influence cytokine gene expression and interferon signalling pathways during FHV-1 infection.

Comparative analysis between field and vaccine strains showed distinct host pathways regulations associated with cell migration, T-cell activation and innate immunity during infections using the vaccine strain. While the vaccine strain induced more host gene changes, the field strain affected a broader range of host pathways. The similarities and differences in host gene and pathway expression associated with immune cell regulation, between field and vaccine strains, suggests the magnitude of gene expression changes may influence the host response. The vaccine strain may induce more targeted changes in specific host pathways to activate a more targeted immune response. However, the field strain may influence more host functions, resulting in a broader impact on immune responses. These findings indicate

future studies investigating host responses associated with viral strain virulence may inform understanding of altered disease outcomes.

Viral transcripts of the late gene UL32 in the field and vaccine FHV-1 strains showed conflicting results between RNA-sequencing and RT-qPCR analysis. While RNA-sequencing identified potential differences in UL32 transcription, this was not confirmed by RT-qPCR. Transcriptomic analysis using RT-qPCR allows high specificity and sensitivity when analysing gene transcripts of low target numbers [41–43]. The similar growth kinetics between field and vaccine strains highlight the low genetic diversity between clinical and vaccine FHV-1 isolates [11, 12], which suggest factors beyond viral gene transcription may contribute to differences in viral virulence between field and vaccine FHV-1 strains. While the attenuation and antigenic difference of the F2 strain is poorly understood, the UL32 gene is conserved amongst herpesviruses and has roles in the cleavage and packaging of viral DNA. Previous HSV-1 transcriptomic study whichgrouped overlapping co-terminal genes into one transcriptional unit to compare viral gene transcription between different HSV-1 strainsshowed distinct viral gene expression patterns between HSV-1 strains in neuronal and epithelial cells [37]. However, by combining genes, this approach may overlook differences in individual gene expressions within the transcriptional unit that contribute to strain-specific host responses. Future studies can use the findings in this study to analyse specific gene expressions at various timepoint across the viral replication cycle or in other cell types, such as primary respiratory cells, to explore strain-specific differences in infection phenotypes.

Conclusions

This study characterised the host and viral transcriptomic profiles of FHV-1 infections in vitro using field and vaccine strains. By comparing the gene expressions between FHV-1 strains that differ in virulence, the findings in this study demonstrate the different host responses associated with viral strain virulence. Investigating the transcriptomic response to FHV-1 infection can inform our understanding of variations in host and viral factors contributing to disease outcomes, which may inform future vaccine attenuation strategies. However, future transcriptomic studies in other systems, such as respiratory tissue explant systems or in vivo infections, will be needed to provide a comprehensive understanding of host responses to FHV-1.

Abbreviations

AGRF	Australian Genome Research Facility
CPE	Cytopathic effects
CPM	Counts per million
CRFK	Crandell- Rees feline kidney
DMEM	Dulbecco's Modified Eagle basal media
FBS	Foetal bovine serum
FCV	Feline calicivirus
FDR	False discovery rate
FHV-1	Varivellovirus felidalpha-1
FVR	Feline viral rhinotracheitis
GO	Gene ontology
HEPES	N-2-hydroxyethylpiperazine-N'-2- ethanesulfonic acid
HSV-1	Herpes simplex virus type 1
h.p.i.	Hours post-infection
LFC	Log_2 fold change
MHC	Major histocompatibility complex
M.O.I.	Multiplicity of infection
N/A	Not applicable
ORFs	Open reading frames
PBS	Phosphate-buffered saline solution
PCA	Principal component analysis
RIN	RNA integrity numbers
$TCID_{50}$	Median tissue culture infective dose
TPM	Transcripts per million
URTD	Upper respiratory tract disease

Supplementary Information

The online version contains supplementary material available at https://doi.org/10.1186/s12985-025-02722-w.

Supplementary Material 1

Supplementary Material 2

Supplementary Material 3

Supplementary Material 4

Acknowledgements

The authors would like to acknowledge Paola Vaz for providing the FHV-1 isolates for this study and the Asia-Pacific Centre for Animal Health research group for supporting this project.

Author contributions

EK performed the experiments, bioinformatics and analysed the transcriptomic data in this study. ARL, CAH and JMD designed the project and offered laboratory advice. ARL provided the cells used in this study. All authors contributed to the editing and revision of the final manuscript.

Funding

No funding.

Data availability

The datasets generated in this study have been desposited in the GenBank repository with BioProject accession number PRJNA1082348. https://www.ncbi.nlm.nih.gov/bioproject/PRJNA1082348/.

Declarations

Ethics approval

Not applicable.

Competing interests

The authors declare no competing interests.

Received: 5 February 2025 / Accepted: 2 April 2025
Published online: 16 April 2025

References

1. Gatherer D, Depledge DP, Hartley CA, Szpara ML, Vaz PK, Benkő M et al. ICTV virus taxonomy profile: herpesviridae 2021. J Gen Virol. 2021;102(10).

2. Gaskell RM, Dennis PE, Goddard LE, Cocker FM, Wills JM. Isolation of felid herpesvirus I from the trigeminal ganglia of latently infected cats. J Gen Virol. 1985;66(Pt 2):391–4.
3. Maes R. Felid herpesvirus type 1 infection in cats: a natural host model for alphaherpesvirus pathogenesis. ISRN Veterinary Sci. 2012;2012:495830.
4. Thiry E, Addie D, Belak S, Boucraut-Baralon C, Egberink H, Frymus T, et al. Feline herpesvirus infection. ABCD guidelines on prevention and management. J Feline Med Surg. 2009;11(7):547–55.
5. Gould D. Feline herpesvirus-1: ocular manifestations, diagnosis and treatment options. J Feline Med Surg. 2011;13(5):333–46.
6. Monne Rodriguez JM, Leeming G, Kohler K, Kipar A. Feline herpesvirus pneumonia: investigations into the pathogenesis. Vet Pathol. 2017;54(6):922–32.
7. Hora AS, Tonietti PO, Guerra JM, Leme MC, Pena HF, Maiorka PC, et al. Felid herpesvirus 1 as a causative agent of severe nonsuppurative meningoencephalitis in a domestic Cat. J Clin Microbiol. 2013;51(2):676–9.
8. Fernandez M, Manzanilla EG, Lloret A, León M, Thibault JC. Prevalence of feline herpesvirus-1, feline calicivirus, Chlamydophila felis and Mycoplasma felis DNA and associated risk factors in cats in Spain with upper respiratory tract disease, conjunctivitis and/or gingivostomatitis. J Feline Med Surg. 2017;19(4):461–9.
9. Monne Rodriguez J, Kohler K, Kipar A. Calicivirus co-infections in herpesvirus pneumonia in kittens. Vet J. 2018;236:1–3.
10. Najafi H, Madadgar O, Jamshidi S, Ghalyanchi Langeroudi A, Darzi Lemraski M. Molecular and clinical study on prevalence of feline herpesvirus type 1 and calicivirus in correlation with feline leukemia and immunodeficiency viruses. Veterinary Res Forum. 2014;5(4):255–61.
11. Lewin AC, Coghill LM, McLellan GJ, Bentley E, Kousoulas KG. Genomic analysis for virulence determinants in feline herpesvirus type-1 isolates. Virus Genes. 2020;56(1):49–57.
12. Vaz PK, Job N, Horsington J, Ficorilli N, Studdert MJ, Hartley CA, et al. Low genetic diversity among historical and contemporary clinical isolates of felid herpesvirus 1. BMC Genomics. 2016;17:704.
13. Rota PA, Maes RK, Ruyechan WT. Physical characterization of the genome of feline herpesvirus-1. Virology. 1986;154(1):168–79.
14. Johnson LR, Maggs DJ. Feline herpesvirus type-1 transcription is associated with increased nasal cytokine gene transcription in cats. Vet Microbiol. 2005;108(3–4):225–33.
15. Bittle JL, Rubic WJ. Immunogenic and protective effects of the F-2 strain of feline viral rhinotracheitis virus. Am J Vet Res. 1975;36(1):89–91.
16. Richter M, Schudel L, Tobler K, Matheis F, Vogtlin A, Vanderplasschen A, et al. Clinical, virological, and immunological parameters associated with superinfection of latently with FeHV-1 infected cats. Vet Microbiol. 2009;138(3–4):205–16.
17. Katoh K, Standley DM. MAFFT multiple sequence alignment software version 7: improvements in performance and usability. Mol Biol Evol. 2013;30(4):772–80.
18. Crandell RA, Fabricant CG, Nelson-Rees WA. Development, characterization, and viral susceptibility of a feline (Felis catus) renal cell line (CRFK). Vitro. 1973;9(3):176–85.
19. Smither SJ, Lear-Rooney C, Biggins J, Pettitt J, Lever MS, Olinger GG. Jr. Comparison of the plaque assay and 50% tissue culture infectious dose assay as methods for measuring filovirus infectivity. J Virol Methods. 2013;193(2):565–71.
20. Afgan E, van den Baker D, Blankenberg D, Bouvier D, Čech M, et al. The galaxy platform for accessible, reproducible and collaborative biomedical analyses: 2016 update. Nucleic Acids Res. 2016;44(W1):W3–10.
21. Blankenberg D, Von Kuster G, Bouvier E, Baker D, Afgan E, Stoler N, et al. Dissemination of scientific software with galaxy toolshed. Genome Biol. 2014;15(2):403.
22. Jalili V, Afgan E, Gu Q, Clements D, Blankenberg D, Goecks J, et al. The galaxy platform for accessible, reproducible and collaborative biomedical analyses: 2020 update. Nucleic Acids Res. 2020;48(W1):W395–402.
23. Martin M. Cutadapt removes adapter sequences from high-throughput sequencing reads. EMBnetjournal. 2011;17(1):10.
24. Lopez JV, Cevario S, O'Brien SJ. Complete nucleotide sequences of the domestic Cat (Felis Catus) mitochondrial genome and a transposed MtDNA tandem repeat (Numt) in the nuclear genome. Genomics. 1996;33(2):229–46.
25. Widmann J, Stombaugh J, McDonald D, Chocholousova J, Gardner P, Iyer MK, et al. RNASTAR: an RNA structural alignment repository that provides insight into the evolution of natural and artificial RNAs. RNA J. 2012;18(7):1319–27.
26. Powell D. drpowell/degust 4.1.1 (4.1.1). Zenodo. 2019 [Available from: https://doi.org/10.5281/zenodo.3501067
27. Ritchie ME, Phipson B, Wu D, Hu Y, Law CW, Shi W, et al. Limma powers differential expression analyses for RNA-sequencing and microarray studies. Nucleic Acids Res. 2015;43(7):47.
28. Law CW, Chen Y, Shi W, Smyth GK. Voom: precision weights unlock linear model analysis tools for RNA-seq read counts. Genome Biol. 2014;15(2):R29.
29. Thomas PD, Ebert D, Muruganujan A, Mushayahama T, Albou L-P, Mi H. PANTHER: making genome-scale phylogenetics accessible to all. Protein Sci. 2022;31(1):8–22.
30. Mi H, Thomas P. PANTHER pathway: an ontology-based pathway database coupled with data analysis tools. Methods Mol Biology. 2009;563:123–40.
31. Mi H, Muruganujan A, Huang X, Ebert D, Mills C, Guo X, et al. Protocol update for large-scale genome and gene function analysis with the PANTHER classification system (v.14.0). Nat Protoc. 2019;14(3):703–21.
32. Gao C, Chen L, Tang SB, Long QY, He JL, Zhang NA, et al. The epigenetic landscapes of histone modifications on HSV-1 genome in human THP-1 cells. Antiviral Res. 2020;176:104730.
33. Conn KL, Hendzel MJ, Schang LM. The differential mobilization of histones H3.1 and H3.3 by herpes simplex virus 1 relates histone dynamics to the assembly of viral chromatin. PLoS Pathog. 2013;9(10):1003695.
34. Cliffe AR, Knipe DM. Herpes simplex virus ICP0 promotes both histone removal and acetylation on viral DNA during lytic infection. J Virol. 2008;82(24):12030–8.
35. Van Opdenbosch N, Van de Favoreel H. Histone modifications in herpesvirus infections. Biol Cell. 2012;104(3):139–64.
36. Wilkinson DE, Weller SK. Recruitment of cellular recombination and repair proteins to sites of herpes simplex virus type 1 DNA replication is dependent on the composition of viral proteins within prereplicative sites and correlates with the induction of the DNA damage response. J Virol. 2004;78(9):4783–96.
37. Mangold CA, Rathbun MM, Renner DW, Kuny CV, Szpara ML. Viral infection of human neurons triggers strain-specific differences in host neuronal and viral transcriptomes. PLoS Pathog. 2021;17(3):1009441.
38. Vyas D, Patel M, Wairkar S. Strategies for active tumor targeting-an update. Eur J Pharmacol. 2022;915:174512.
39. Wang J, Wang S, Chen L, Tan J. SCARA5 suppresses the proliferation and migration, and promotes the apoptosis of human retinoblastoma cells by inhibiting the PI3K/AKT pathway. Mol Med Rep. 2021;23(3):202.
40. Montagnaro S, Longo M, Pacilio M, Indovina P, Roberti A, De Martino L, et al. Feline herpesvirus-1 down-regulates MHC class I expression in an homologous cell system. J Cell Biochem. 2009;106(1):179–85.
41. Litster A, Wu CC, Leutenegger CM. Detection of feline upper respiratory tract disease pathogens using a commercially available real-time PCR test. Vet J. 2015;206(2):149–53.
42. Yang D-K, Kim H-H, Park Y-R, Yoo JY, Choi S-S, Park Y, et al. Isolation and molecular characterization of feline herpesvirus 1 from naturally infected Korean cats. J Bacteriol Virol. 2020;50(4):263–72.
43. Mazzei M, Vascellari M, Zanardello C, Melchiotti E, Vannini S, Forzan M, et al. Quantitative real time polymerase chain reaction (qRT-PCR) and RNAscope in situ hybridization (RNA-ISH) as effective tools to diagnose feline herpesvirus-1-associated dermatitis. Vet Dermatol. 2019;30(6):491–147.

Publisher's note